Accepted Manuscript

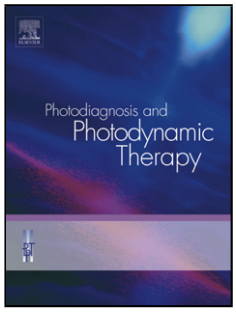

Title: Photochemotherapy using natural anthraquinones: rubiadin and soranjidiol sensitize human cancer cell to die by apoptosis

Author: Natalia Belén Rumie Vittar Laura Comini Ivana M. Fernández Elizabeth Agostini Susana Núñez Montoya José Luis Cabrera Viviana Alicia Rivarola

PII: S1572-1000(14)00009-X
DOI: http://dx.doi.org/doi:10.1016/j.pdpdt.2014.02.002
Reference: PDPDT 531

To appear in: *Photodiagnosis and Photodynamic Therapy*

Received date: 31-10-2013
Revised date: 7-2-2014
Accepted date: 8-2-2014

Please cite this article as: Natalia Belén Rumie VittarLaura CominiIvana M FernándezElizabeth AgostiniSusana Núñez MontoyaJosé Luis CabreraViviana Alicia Rivarola Photochemotherapy using natural anthraquinones: rubiadin and soranjidiol sensitize human cancer cell to die by apoptosis (2014), http://dx.doi.org/10.1016/j.pdpdt.2014.02.002

Title: PHOTOCHEMOTHERAPY USING NATURAL ANTHRAQUINONES: RUBIADIN AND SORANJIDIOL SENSITIZE HUMAN CANCER CELL TO DIE BY APOPTOSIS.

Authors: Natalia Belén Rumie Vittar[1*], Laura Comini[2*], Ivana M Fernández[1], Elizabeth Agostini[1], Susana Núñez Montoya[2], José Luis Cabrera[2], and Viviana Alicia Rivarola[1]

[1]Departamento de Biología Molecular, Facultad de Ciencias Exactas Físico-Químicas y naturales, Universidad Nacional de Río Cuarto, CP 5800 Río Cuarto, Córdoba, Argentina.
[2]Farmacognosia, Departamento de Farmacia, Facultad de Ciencias Químicas (IMBIVCONICET), Ciudad universitaria, Universidad Nacional de Córdoba, CP 5000 Córdoba, Argentina.

E-mail address:

nrumievittar@exa.unrc.edu.ar (Rumie Vittar NB)

lcomini@fcq.unc.edu.ar (Comini L)

ivimar2002@yahoo.com.ar (Fernandez IM)

eagostini@exa.unrc.edu.ar (Agostini E)

sununez@fcq.unc.edu.ar (Núñez Montoya S)

jcabrera@fcq.unc.edu.ar (Cabrera J)

vrivarola@exa.unrc.edu.ar (Rivarola VA)

Corresponding author: Tel.: +543584676437, Fax: +543584676232

E-mail address: vrivarola@exa.unrc.edu.ar (Rivarola VA)

Address: CP 5800 Río Cuarto, Córdoba, Argentina

* N.B. Rumie Vittar and L. Comini contributed equally to this work.#

#

1. INTRODUCTION

Photodynamic therapy (PDT) or photochemotherapy is a clinically approved, minimally invasive therapeutic procedure that can exert a selective cytotoxic activity toward malignant cells. The procedure involves administration of a photosensitizing agent (PS) followed by irradiation at a wavelength corresponding to an absorbance band of the sensitizer. This creates the photodynamic reaction which is tumor and vascular ablative (Agostinis et al 2011, Allison and Moghissi 2013).

Diverse natural PSs as hypericins, hypocrellins and pheiochrome showed great activity under PDT protocols (Stockert et al 2004). Other derivatives such as paclitaxel and aloe-emodin occasioned interesting photodynamic effect on tumor cell cultures (Lee et al 2010, Zhang et al 2010).

Due to the great demand of vegetal compounds that has the international trade; the plant cell cultures represent new technologies that extend and enhance the usefulness of plants as sources of natural valuable compounds (Acurero 2011).

One type of *in vitro* cultures are the calli, characterized for being a disorganized mass of undifferentiated tissue with active dividing cells (Vanisree et al 2004). This biotechnological tool has been mainly used for the synthesis and extraction of bioactive natural products, such as therapeutic drugs.

Heterophyllaea pustulata Hook f. (Rubiaceae) is a phototoxic plant that grows in the Andean northwest of Argentina. The ingestion of different parts of the plant produces toxic effect such as dermatitis and blindness on bovine, goat and equine cattle (Hansen and Martiarena 1967, Aguirre and Neumann 2001). We have reported previously that anthraquinones (AQs) isolated from leaves and stem of *H. pustulata* exhibited photosensitizing properties by generation of singlet oxygen and/or superoxide anion radical (Núñez Montoya *et al* 2005). In other study, we observed that these AQs present increased photodynamic activity on cancerous cells (Comini et al 2011). In addition, we showed that AQs occasioned photosensitization on Balb/c mice (Núñez Montoya et al 2008). In PDT, the current studies are centralized in the characterization of new synthetic and/or natural drugs that once photoactivated induce apoptosis, necrosis or autophagy (Rumie Vittar et al 2010, Sharma and Davids 2012).

Apoptotic cell death is morphologically characterized by chromatin condensation, cleavage of chromosomal DNA into internucleosomal fragments, cell shrinkage, membrane blebbing, formation of apoptotic bodies without plasma membrane breakdown. At the biochemical level, apoptosis entails the participation of caspases, a family of cysteine dependent aspartate-specific proteases, which act in two main converging pathways, extrinsic and intrinsic and this signaling finish with the activation of executioner caspases, caspase-3 and -7 that cleavage and inactive defined substrates implicated in cells protection as (ADP-ribose) polymerase (PARP). In contrast, apoptosis may occur by caspase-independent pathway implicating apoptosis inducing factor (AIF) and endonuclease G (Endo G) (Orrenius et al 2011). In addition to caspases, other proteases are implicated in

the cellular death, such as calpains. These proteases belong to a family of calcium activated cystein proteases and have function in a wide variety of biological processes, including cell division, differentiation, migration, and apoptosis (Kroemer et al 2009).

While the majority of approved PDT protocols treat superficial lesions of skin and luminal organs, interstitial and intra-operative approaches have been investigated for the ablation of a broad range of superficial or bulky solid tumors such as breast cancer (Huang et al 2008, Master et al 2013). Breast cancer is the most common women's cancer in the world. In recent years possibilities of PDT using in breast cancer treatment are analyzed (Płonka and Latocha 2012). In this investigation, our studies were mainly focused on the efficacy's assessing of natural photosensitizers, Rubiadin and Soranjidiol obtanined from *H. pustulata* callus cultures, on human breast cancer cell lines. The viability, AQs intracellular localization and phototoxicity, exploring the cell death mechanism induced on cancer cells by the AQ-PDT treatment are analyzed. Also an alternative PDT combination, on which the synergic, antagonic or additive Rubiadin- and Soranjidiol- effect was examined.

2. MATERIALS AND METHODS

2.1. Recollection and *in vitro* germination of *H. pustulata* seeds

The seeds of *Heterophyllaea pustulata* were collected in Salta province, Argentina, in June 2008. The material was identified by Prof. Dr. Gloria Barboza (Instituto Multidisciplinario de Biología Vegetal, Consejo Nacional de Investigaciones Científicas y Técnica, Universidad, Nacional de Córdoba (IMBIV, CONICET, UNC). The seeds were surface disinfected by immersion in 70% ethanol for 1 min followed by treatment with 30% sodium hypochlorite (NaClO) for 5 min. To remove the traces of chlorines, they were washed twice with sterile distilled water. Then, seeds were transferred to Murashige and Shoog (MS) medium (Murashige and Skoog 1962) supplemented with vitamins solution pH 5.7-5.8 and they were incubated at 28ºC in a culture chamber under a 16 h photoperiod.

2.2. Callus induction from different explants of *H. pustulata*

Leaf, root and stem explants derived from plants of three month age were excised longitudinally and placed on basal MS medium supplemented with 1 mg/L of 2,4-dichlorophenoxyacetic acid (2,4-D, Sigma) for inducing callus. They were incubated in darkness in growth chamber at 28ºC. To maintain the callus culture, the proliferated calli were regularly subcultured every 3 week intervals on fresh medium with the same composition supplemented with antioxidant solution [2 mM L-glutamine (Sigma), 0.285 mM L- ascorbic acid (Sigma) and 0.26 mM citric acid (Sigma)].

2.3. Quantitative analysis of anthraquinones in callus cultures

Calli were dried in stove at 50°C and the AQs were obtained for successively benzene extraction at room temperature. The extracts obtained in each experiment were dried under reduced pressure and dissolved in methanol (MeOH; HPLC grade). All samples were filtered through a 0.2 mm cellulose acetate membrane filter (Micro Filtration System) before HPLC analysis. HPLC analysis (qualitative and quantitative) was performed on a Varian Pro Star chromatograph (model 210, series 04171), equipped with a UV–Vis

detector and a Microsorb-MV column 100-5 C18 (250 x 4.6 mm i.d., Varian). The mobile phase was MeOH–H2O (8:2) at constant flow (1 mL/min) and the injection volume was 20 µl. The detection was performed at the wavelength of 269 nm. The AQs identification was carried out by comparison of the HPLC retention times (tR) with the corresponding standards Rubiadin and Soranjidiol under the same chromatographic conditions. The AQs standards were obtained from Nunez-Montoya et al 2003. Each AQ, were quantified through the external calibration method (Núñez et al. 2008). Using the calibration curves, the concentration of each AQ in extract fraction was calculated by interpolating the area under each peak (AUP) for each compound. The seven pointed constructed curves (n=3) were linear (correlation coefficients >0.99).

2.4. Cell culture

MCF-7c3 human cancer cells transfected with retroviral vector pBabepuro codified cADN human CPP32 (procaspase 3) was provided by Dr. CJ Froelich of Northwestern University, Evanston, IL, USA. Cells were used as human cancer model and for to assess the possibilities of PDT using in solid tumors such as breast cancer. Cultured were cultivated in Dulbecco´s modified Eagle medium (DMEM, Gibco BRL) supplemented with 10% v/v fetal calf serum (Gibco BRL), 1% glutamax (Gibco BRL), 1% antibiotic/antimycotic solution (Gibco BRL) and 1% of piruvate (Hyclone®) and maintained in a humidified atmosphere at 37°C and 5% CO_2.

2.5. Photodynamic activity

Cells were seeded at $2x10^4$cells/mL in multi-well plates and incubated in humidified atmosphere comprising 95% air and 5%CO_2. When the cells reached 85% confluence were immediately treated with 100 µM of AQ (stock solution AQ dissolved in phosphate buffered saline, AQPBS), a not toxic dark concentration. We selected for irradiation the absorption bands of AQs between 410 and 420 nm (Comini et al 2011). The irradiation system comprised a non halogen actinic lamp (Phillips 24 V/150 W, 380–480 nm, 1.19 mW/cm^2 (Radiometer Laser Mate-Q, Coherent) with a maximum of 420 nm. All irradiations were performed at room temperature. The light dose delivered for the PDT treatments were 0.35, 0.7 and 1 J/cm^2. Once the treatment finished, the AQ solution was replaced by fresh medium and incubated in a humidified atmosphere at 37°C and 5% CO_2 for 24 h. Light control was carried out in parallel. Concluded the treatments, cellular viability was determined by the reduction of the tetrazolium salt MTT (3-(4,5-dimethylthiazolil-2)-2,5-diphenyltetrazolium bromide-Sigma) (Denizot and Lang 1986).

2.6. Intracellular localization

Cells ($2x10^4$ cells/mL) grown in dish culture plates were treated with AQ maximum concentration (no toxic in dark condition) dissolved in PBS during 90 min at 37°C. After treatment, solution was recollected and the monolayer was rinsed and fixed with formaldehyde vapors for 2 min. Then, they were treated with 1% aluminum potassium sulfate (AlK(SO4), Sigma) for 5 min which was used with the purpose to intensify the AQ fluorescence. Intracellular localization was visualized under fluorescence microscopy.

2.7. Nuclear morphology

Once the photodynamic treatment finished, the detached cells were recollected and centrifuged twice at 1000 rpm for 10 min to obtain pellet. Then were fixed with cold methanol during 5 min and stained with 1 µg/mL Hoechst 33258 (Ho, Sigma) for 5 min.

Attached cells were washed with PBS, fixed with 4% formaldehyde for 15 min and then permeabilized with 0.1% Triton X-100/PBS for 5 min at room temperature. Finally, the cells were stained with 1 μg/mL Ho for 3 min and rinsed several times with distilled water. To corroborate the apoptotic cells, acridine orange (AO, Sigma) was used. Detached cell were centrifuged at 2000 rpm for 2 min and the resultant pellet was stained with 10 μg/mL AO for 1 min whereas attached cells were washed with PBS and stained with AO, and then rinsed to remove any remaining. Nuclear morphology was visualized using a fluorescence microscope.

2.8. Apoptosis analysis

Cellular apoptosis was evaluated using a Cell Death Detection ELISA Plus kit (Roche). This assay allows to measure mononucleosomes and oligonucleosomes from cell lysates using monoclonal antibodies targeting DNA and histones in a quantitative photometric sandwich enzyme immunoassay. MCF-7c3 cells were treated with 100 μM of Rubiadin or Soranjidiol and immediately irradiated with 1 J/cm^2. Then, treatment solution was replaced for fresh medium and cells were incubated at 37°C. Cell samples were recollected 6, 14 and 24 h after photodynamic treatment. In parallel, light and dark controls were performed. Apoptotic index was calculated for relation between treated cells respect control cells.

2.9. Western blot analysis

Cells were incubated with or without 100 μM Rubiadin or Soranjidiol and irradiated with 1 J/cm^2. Then treatment solution was replaced by fresh medium and the monolayer was incubated at 37°C. Cell samples were obtained at different times after treatment (1, 3 and 6 h). Attached and detached cells were harvested and centrifuged at 2000 rpm for 5 min. Cell pellets were suspended in lysis buffer RIPA (10 mM Tris–HCl, pH 7.2, 150 mM NaCl, 1% Triton X-100, 0.1% sodium dodecyl sulfate, 1% sodium deoxycholate, 5 mM EDTA, protease inhibitor (1 tablet) and homogenized with syringe. Samples were placed on ice for 15 min. Protein concentration was determined using the BCA kits.

Equal amounts of protein (40 μg/mL) were separated by electrophoresis on a SDS-PAGE gel and then transferred to a polyvinylidene difluoride (PVDF) membrane (Sigma-Aldrich). Blots were soaked in blocking buffer (5% non-fat dry milk) during 2 h, and then incubated with specific primary antibodies against caspase-3 (Cell signaling), PARP (Santa Cruz), calpain (Cell Signaling) and α-tubulin (Sigma) overnight at 4°C. After exposure, membranes were washed with PBS-0.1% Tween, and treated with peroxidase conjugated secondary antibody (Cell Signaling) for 2 h. Proteins were visualized using an enhanced chemiluminescence detection kit (ECL Kits; Amersham Life Science).

2.10. DNA fragmentation analysis

MCF-7c3 cells were treated with 100 μM Rubiadin or Soranjidiol and irradiated with 1 J/cm^2, after treatment AQ solution was replaced for fresh medium. Cells were maintained at 37°C for 6 h. Concluded photodynamic treatment, cellular samples were harvested with trypsin-EDTA (Gibco) and washed with ice-cold PBS by centrifugation at 10000 rpm for 2 min. Cell pellets were then suspended in 200 μl lysis buffer (50 mM Tris–HCl, 100 mM NaCl, 4 mM EDTA, 0.5% SDS, pH 8) with 100 μg proteinase k (stock solution 20 mg/mL,

Sigma) and were incubated at 55°C for 2 h. After addition of 1 M potassium acetate and 250 µl chloroform during 30 min on ice, the samples were centrifuged at 12000 rpm for 8 minutes at 4°C. The DNA was extracted and precipitated with 2.5 vol ethanol at -20°C for 30 minutes, and centrifuged at 12000 rpm for 20 minutes. Pellets were washed with 70% ethanol and centrifuged at 12000 rpm for 5 minutes. Pellets were incubated with 0.5% TAE buffer (1X solution: 40 mM Tris, 20 mM acetic acid, and 1 mM EDTA) and RNAsa (1 mg/mL, Invitrogen) for 1 h at 37°C and stored at -20°C. Then, separation by electrophoresis was performed on 1.7% agarose containing ethidium bromide. The DNA bands were examined using a UV Transilluminator Imaging System. In parallel, controls were realized.

2.11. Phototherapeutic combinations

MCF-7c3 cells ($2x10^4$ cells/mL) were treated with different Rubiadin and Soranjidiol combinations (1, 50 and 100 µM), and immediately they were irradiated with 1 J/cm2. After treatment the cells were maintained with fresh medium in a humidified atmosphere at 37°C and 5% CO_2 for 24 h. Corresponding controls were realized under the same conditions. Cellular viability was determined by MTT assay. Drug interaction and CI were determined using median-effect analysis according to the method of Chou and Talalay (Chou and Talalay 1984). Combination index (CI) was determined from the CIisobologram method using the computer program developed by Chou and Martin (Chou and Martin 2005). The three possibilities: CI < 1, CI = 1, and CI > 1, indicated synergy, additive effect, and antagonism, respectively.

2.12. Photodynamic effect of commercial anthraquinones

MCF-7c3 cells were seeded at 2 $x10^4$ cells/mL in multi-well plates. When cells presented 85% confluence, they were incubated with different commercial anthraquinones (1,2-dihydroxyanthraquinone called Alizarin and 1,2,4-Trihydroxyanthraquinone called Purpurin) concentrations (1, 50 and 100 µM) and immediately were irradiated with 1 J/cm^2. After phototherapeutic treatment anthraquinone solution was replaced for fresh medium, and cells were maintained in a humidified atmosphere at 37°C and 5% CO_2 for 24 h. Corresponding controls were realized under the same conditions. Cellular viability was determined by MTT assay.

3. RESULTS AND DISCUSSION

3.1. *In vitro* seed germination of *Heterophyllaea pustulata*

In this study, *H. pustulata* seeds were germinated on MS medium without phytohormones. Ideal plants were obtained after 3 months of grown on 0.25% MS medium under a photoperiod of 16 h light and 8 h dark (Figure 1A). Only leaves and stems exhibited formation of a cellular amorphous orange mass after 15 days of incubation on MS basal medium containing 1.0 mg/l 2,4-D (Figure 1B). HPLC analysis revealed presence of Rubiadin and Soranjidiol in callus cultured on the MS basal medium supplemented with 1.0 mg/l of 2,4-D (Figure 1C), their levels were significantly higher than in leaves, stems and roots cultures corresponding to 27 and 33.4%, respectively (Table 1). Continuous

subcultures of the callus showed oxidative phenotype to the second subculture but this phenotype was reverted. Content and concentration of AQs were similar to that determined in the initial callus (Figure 1D, Table 2). Based on our results, we suggest that AQs production in callus cultures derived from the original plan *H. pustulata* would be a better alternative than the extraction of these compounds from field cultivated plants.

3.2. Effect of photoactivated AQs on cancer cell viability

Our previous report showed that Rubiadin and Soranjidiol resulted innocuous in dark condition and further activation with visible light induced cytotoxicity on cancer cells (Comini et al 2011). In this study, we wondered to evaluate the cellular viability effect of different AQs activating light energy (0.35, 0.7 and 1 J/cm^2). As shown in Figure 2A both AQs, Rubiadin and Soranjidiol, were photochemically active in light dose-dependent manner. The photosensitizing ability of Soranjidiol appeared to be more effective than Rubiadin, exhibiting a LD50 value with 0.49 J/cm^2 irradiation energy, and significant 94% cell killing with 1 J/cm^2. Instead, Rubiadin showed a LD50 value with 0.66 J/cm^2 light dose and a 76 % cell reduction at maximum light activation.

Cell morphology was not affected by light or AQs alone compared to untreated controls (data not shown). This fact was confirmed by toluidine blue stained preparations. Regarding photodynamic treatment, cells displayed altered morphology, showing higher number of cells with swollen membrane and irregular cytoplasm. The phototoxic effect observed is thought to be responsible for the rounding-up process. Rubiadin-PDT photodamage may cause more injury on MCF-7c3 cells (Figure 2B). Based on our previous studies, we suggest that cellular survival diminished in a light dose-dependent manner could be related to the ROS production under AQ light activation (Núñez Montoya et al 2005).

3.3. AQs intracellular localization

The subcellular localization of the PS is one of the crucial factors in determining the type of cell death due to the chemically generated ROS responsible of the oxidative damage. Previously, we have demonstrated that Rubiadin and Soranjidiol produced ROS and were incorporated into cancerous cells (Núñez Montoya et al 2005, Comini et al 2011). In this study, we have shown that Rubiadin and Soranjidiol can readily pass through cell membrane, accumulated the most within cells and exhibited red fluorescence mainly in the cytoplasmic region (Figure 3). Cultures did not provide evidence for AQ penetration into the cell nucleus. The subcellular AQs pattern allowed us to assume a minimal mutagenesis risk which permitted us to continue the studies.

3.4. AQs sensitize tumor cells leading to apoptosis

PDT-mediated cell death was assessed by Hoechst/AO and the degree of apoptosis quantified by counting condensed and fragmented nuclei post-photosensitization. As illustrated in Figure 4, MCF-7c3 control cells (non-irradiated non-treated) had a normal nuclear morphology, while those exposed to PDT (Rubiadin or Soranjidiol, 100 μM + 1 J/cm^2) revealed profound nuclei alterations. Nuclear condensation and DNA fragmentation were detected in cells under PDT schedule (Rubiadin-PDT or Soranjidiol-PDT).

Despite the many characteristics of apoptotic cells, Rubiadin-PDT exhibited more percentage of cells with fragmented DNA than Soranjidiol-PDT (77 and 60% respectively), indicating that the treatment can rapidly triggered late apoptosis stage (Table 3). We did not observe any significant difference in nuclear cell morphology between non-irradiated AQ-treated cells and irradiated untreated cells.

To further confirm apoptosis, treated cells were analyzed with the mono- and oligonucleosomes induction time course by ELISA (Fig. 5). Rubiadin- and Soranjidiol-PDT increase the apoptotic index by nearly 7-fold compared to control at 6 h from treatment indicating the appearance of mono- and oligonucleosomes. However, solely Soranjidiol-PDT sustained the level within first 14 h.

Apoptotic DNA is a valuable marker of apoptosis because it is a late "point of no return" (Rumie Vittar et al 2010, Hooker et al 2012). For this reason, we further investigated the AQs-PDT-induced DNA degradation pattern. As shown in Figure 6, Rubiadin-PDT DNA laddering actually turned out to be very strong compared to a positive control like STS-treated MCF-7c3 cells. However, Soranjidiol-PDT failed to induce DNA laddering pattern like positive control. These results provided convincing data showing that Rubiadin- and Soranjidiol-PDT could induce apoptosis in MCF-7c3 cells, but the molecular events that degrade their DNA may do not be similar.

To analyze the molecular mechanism underlying apoptosis, we determined caspase-3 activation and detection of intact and cleaved poly-ADP ribose-polymerase that binds at DNA strand breaks. As shown in Fig. 7A, Rubiadin-PDT strongly stimulated the caspase-3 activation (17 kDa fragment) as soon as 1 h post-irradiation which correlated with cleavage of PARP (89 kDa). These data demonstrated that Rubiadin-PDT triggered an early apoptotic signal that culminated in DNA internucleosomal fragmentation mediated by caspase-3. In contrast, we did not observe pro-caspase-3 cleavage after treatment with Soranjidiol-PDT (Figure 7B). Surprisingly, we found that calpain (76 kDa) but not caspase-3 had effect on PARP cleavage (from 116 kDa to 60 kDa and 24 kDa fragments), suggesting that cells undergo a non-canonical apoptotic cell death.

Previously, we have reported non oligonucleosomal DNA fragmentation after PDT and a noticeable stage I chromatin condensation and large-scale (50 kb) DNA fragmentation (Rumie Vittar et al 2010). More surprising is the fact that upon Soranjidiol-PDT apoptotic stimuli, MCF-7c3 cells did display neither internucleosomal-size DNA (180 bp multiples) nor large-size DNA fragment (50-300 kb). Several research groups have detected large DNA fragments during apoptosis and they proposed that large DNA fragmentation occurs before internucleosomal DNA cleavage and these large fragments serve as precursors for the smaller DNA fragments (Bortner et al 1995). Consistent with these reports, our observations also suggest that under Soranjidiol-PDT treatment the internucleosomal DNA cleavage appears delayed. In this regard, a non-canonical mechanism involving caspase-independent cell death and calpain could explain the delayed DNA degrading into small fragments.

3.5. Photocytotoxic effect of Rubiadin in combination with Soranjidiol

Combination of antineoplastic drugs is used, in order to reduce the possible resistance of tumor cells and minimize unwanted side effects. Due to interesting photodynamic activity occasioned by Rubiadin and Soranjidiol on MCF-7c3 cells, we examine their combined effect in order to reduce the AQ dose applied. First, we evaluated the tumor cell viability in a wide range of compounds concentrations, comparing their effects with commercial AQs (Figure 8A). Interestingly, our results indicated that MCF-7c3 cells were highly sensitive to a Rubiadin- and Soranjidiol-PDT treatment compared to commercial anthraquinones (Alizarin or 1,2- dihydroxyanthraquinone and 1,2,4-Trihydroxyanthraquinone, commonly called Purpurin) under the same therapeutic conditions (Figure 8B). In order to test the synergistic effect on inducing tumor cell death, we combined Rubiadin and Soranjidiol in different ratios (1:1, 1:50, 1:100, 50:1, 50:50, 50:100, 100:1, 100:50 and 100:100) and performed MTT assay (Figure 8C). The graphs and combination indexes from the compuSyn software analysis (Figure 8C and Table 4) clearly show that the effects of these combined natural compounds were antagonistic or synergistic. The data suggest that doses below 50 μM of Rubiadin are not possible with the combined Soranjidiol regimens, but these agents can be used in combination for an augmented cytotoxic effect under the synergic conditions. Regarding the impact on cell viability, the combined treatment of 50 μM Rubiadin + 50 μM Soranjidiol-PDT exhibited an attractive inhibitory effect. From data analysis, we suggest that Rubiadin and Soranjidiol could be used in synergic PDT protocols, one of them with a real therapeutic potential for to be used in tumor treatment.

4. CONCLUSIONS

We presented experimental evidence that support the antitumor effect of Rubiadin- and Soranjidiol-PDT *in vitro*. Thus, our studies support an approach for intracellular signals triggering apoptotic cell death. Furthermore, our studies reveal a novel cancer treatment using the photodynamic combination of Rubiadin and Soranjidiol, and we propose that this combination might represent an efficient therapeutic strategy. Further studies are definitely necessary to validate the real potential in the context of PDT using *in vivo* tumors.
Moreover, we have standarized the obtention of callus cultures with high content of AQs, and in the future this *in vitro* strategy might be used to perform a large-scale production process.

ACKNOWLEDGEMENTS

This research was supported by Consejo Nacional de Investigación Científica y Tecnológica (CONICET), Agencia FONCyT (PICT) and Secretaría de Ciencia y Técnica (SeCyT) of Universidad Nacional de Río Cuarto (UNRC).

REFERENCES

Acurero A, 2011, Bioagro. 23(2), 79-86.

Agostinis P, Berg K, Cengel K, Foster T, Girotti A, Gollnick H, Hahn S, Hamblin M, Juzeniene A, Kessel D, et al., 2011, CA Cancer J Clin. 61(4), 250–281.
Allison RR, Moghissi K, 2011, Clin Endosc. 46, 24-29.
Aguirre D, Neumann R, 2001, Medicina Veterinaria. 18(7-8), 487-490.
Bortner CD, Oldenburg NB, Cidlowski JA, 1995, Trends. Cell. Biol. 5(1), 21-26.
Chou TC, Martin N, 2005, ComboSyn: Paramus (NJ).
Chou TC, Talalay P, 1984, Adv. Enzyme. Regul. 22, 27-55.
Comini LR, Fernandez IM, Rumie Vittar NB, Núñez Montoya SC, Cabrera JL, Rivarola VA, 2011, Phytomed. 18, 1093-1095.
Denizot F, Lang R, 1986, J. Immunol. Methods. 89, 271-277.
Hansen EW, Martiarena CA, 1967, Rev. Inv. Agropec. Parol. Anim. 4, 81-112.
Hooker DJ, Mobarok M, Anderson JL, Rajasuriar R, Gray LR, Ellett AM, Lewin SR, Gorry PR, Cherry CL, 2012, Nucleic. Acids. Res. 40, 15-20.
Huang Z, Xu H, Meyers AD, Musani AI, Wang L, Tagg R, Barqawi AB, Chen YK, 2008, Technol Cancer Res Treat. 7(4), 309–320.
Kroemer G, Galluzzi L, Vandenabeele P, Abrams J, Alnemri ES, Baehrecke EH, Blagosklonny MV, El-Deiry WS, Golstein P, Green DR, et al., 2009, Cell. Death. Differ. 16(1), 3-11.
Lee H, Yang WH, Hour MJ, Wu CY, Peng WH, Bao BY, Han PH, Bau DT, 2010, Eur. J. Pharmacol. 648, 50-58.
Master A, Livingston M, Gupta AS, 2013, J Control Release.168(1), 88–102.
Murashige T, Skoog F, 1967, Plant. Physiol. 15, 473-479.
Núñez Montoya SC, Agnese AM, Perez C, Tiraboschi IN, Cabrera JL, 2003, Phytomedicine. 10, 569–574.
Núñez Montoya SC, Comini LR, Rumie Vittar B, Fernandez IM, Rivarola VA, Cabrera JL, 2008, Toxicon. 51, 1409-1415.
Núñez Montoya SC, Comini LR, Sarmiento M, Becerra C, Albesa I, Arguello G, Cabrera JL, 2005, J. Photochem. Photobiol. B. 78, 77-83.
Orrenius S, Nicotera P, Zhivotovsky B, 2011. Toxicol. Sci. 119, 3-19.
Rumie Vittar NB, Awruch J, Azizuddin K, Rivarola V, 2010, Int. J. Biochem. Cell. Biol. 42, 1123-1131.
Schneider-Yin X, Kurmanaviciene A, Roth M, Roos M, Fedier A, Minder E, Walt H, 2009, Photodiagn. Photodyn. Ther. 6(1), 12-18.
Sharma KV, Davids LM, 2012, Cell. Biol. Int. 36, 1261-1266.
Stockert JC, Juarranz A, Villanueva A, Nonell S, Horobin RW, Solterman AT, Durantini AN, Rivarola V, Colombo L, Espada J, et al., 2004, Curr. Top. Pharmacol. 8(2), 187-217.
Vanisree M, Lee CY, Lo SL, Nalawade S, Lin C, Tsay HS, 2004, Bot. Bull. Acad. Sin. 45, 1-22.
Zhang ZF, Huang Y, Shi X, Wang RX, Lin XY, Lin XD, Zheng H, Li LB, 2010, J. South. Med. Univ. 30(6), 1310-1315.

LEGENDS FOR FIGURES

Figure 1. Germination of *Heterophyllaea pustulata*, callus induction and anthraquinones production. (A) Plant of *H. pustulata* grown on MS medium after 25 days maintained at 28ºC in room culture with 16 h photoperiod. (B) Callus formation from leaves and stems in MS medium supplemented with 1.0 mg/l 2,4-dichlorophenoxyacetic acid, 15 days culture old. (C) HPLC bencenic extract reveal anthraquinones production from different vegetal explants. (D) HPLC anthraquinones pattern in *H. pustulata* oxidized callus.

Figure 2. Rubiadin or Soranjidiol-PDT inhibited cancer cells survival in light dose dependent manner. (A) Cells were treated with 100 μM Rubiadin or Soranjidiol and exposed to different light energy (0.35, 0.7 and 1 J/cm^2). The related cell viability was assessed at 24 h by MTT. Data are represented as the mean ± S.D. obtained from three independent experiments. (B) MCF-7c3 cells were treated with 100 μM Rubiadin or Soranjidiol and irradiated with 1 J/cm^2. Changes in cell morphology were assessed at 24 h post-PDT. Phase contrast (PC). Toluidine Blue (TB).

Figure 3. Subcellular localization of Rubiadin and Soranjidiol. Cells were treated with 100 μM by 90 min and then were observed under fluorescence microscopy. (A) Control; (B) Rubiadin fluorescence; (C) Soranjidiol fluorescence. Scale bar: 10 μm.

Figure 4. Rubiadin- or Soranjidiol-PDT induced apoptotic cell death. MCF-7c3 cells treated with PDT regimen (100 μM AQ + 1 J/cm^2) were fixed and subjected to Hoechst (Ho) or acridine orange (AO) staining to detect apoptotic nuclei. Figures are representative data collected from three independent experiments.

Figure 5. AQ-PDT apoptosis time course in human cancer cell line. Cell were treated with 100 μM Rubiadin (A) or Soranjidiol (B) and exposed to 1 J/cm^2. Apoptosis was examined at 6, 14 and 24 h post-PDT by determining nucleosomal DNA fragmentation. The last bar corresponds to positive control DNA-Histone-Complex. Data are represented from three independently performed experiments.

Figure 6. DNA fragmentation after Rubiadin- or Soranjidiol-PDT. DNA fragmentation was assessed by a DNA laddering experiment performed on MCF-7c3 cells at 6 h post-PDT. The positive control was MCF-7c3 cells treated with 1 μM staurosporine for 6 h (STS).

Figure 7. Molecular apoptotic profile of Rubiadin- or Soranjidiol-PDT. (A) Caspase-3 and PARP cleavage was assessed in MCF-7c3 cells treated with Rubiadin (100 μM + 1 J/cm^2). β-Actin is used as loading control. (B) Caspase-3, PARP, calpain and α–tubulin levels were assessed in MCF-7c3 cells treated or not with 100 μM Soranjidiol at various times post-irradiation. STS was used as caspase-3 and PARP cleavage positive controls.

Figure 8. Rubiadin and Soranjidiol combination synergistically decrease cancer cell viability. (A) MCF-7c3 cells were exposed to different AQs concentrations. Cell viability assessed at 24 h by MTT assay in cell treated with Rubiadin- PDT (left column graph) or Soranjidiol-PDT (right column graph). (B) Photodynamic effect induced by Alizarin and Purpurin. Cells were treated with Alizarin (left column graph) or Purpurin (right column graph) at different concentrations and irradiated with 1 J/cm^2. (C) Cells treated with different Rubiadin and Soranjidiol-PDT combination (0, 1, 50, 100 μM + 1 J/cm^2). Cell survival was determinate at 24 h. Data are represented as the mean ± S.D. obtained from three independent experiments.

Table 1. Anthraquinones production in callus extract of *H. pustulata*. Anthraquinone quantification from bencenic fraction in root, leaf, stem, and callus. The percentage was calculated by interpolating the area under each peak for Rubiadin and Soranjidiol HPLC profile.

Table 2. Anthraquinones production in oxidized callus extract of *H. pustulata*. Percentage of AQs in bencenic extract obtained from callus was calculated by interpolating the area under each peak for Rubiadin and Soranjidiol HPLC profile.

Table 3. Nuclear morphology after AQs-PDT protocol. Five photographs per well were taken for assessed nuclear morphology by fluorescence microscopy. Non-modified, condensed or fragmented nuclei were qualified and quantified by calculating percentage in each experimental condition.

Table 4. Antagonic and synergic effect of Rubiadin/Soranjidiol combination under PDT protocols. The values were obtained using the software CompuSyn. CI: Combination index for each anthraquinone (CI > 1 antagonic combination, CI < 1 synergic combination). Fa: fraction affected.

Bencenic extract	Rubiadin	Soranjidiol
Root	8.9%	2.7%
Leaf	2.3%	2.6%
Callus	27%	33.4%
Stem	9.7%	14.1%

Table. 1

Table. 2

Bencenic extract	Rubiadin	Soranjidiol
Oxidized callus	31%	35%

Table. 3

Conditions	Non-modified (%)	Condensed (%)	Fragmented (%)
Control	100±5	-	-
Light control	97±5	-	3±1
Rubiadin	100±4.2	-	-
Soranjidiol	98±3.7	2±1.8	-
Rubiadin-PDT	19±4	4±2.1	77±4.5
Soranjidiol-PDT	4±1.5	37±2.2	60±3

Rubiadin dose (μM)	Soranjidiol dose (μM)	Fa	CI	Description
1	1	0.0010	2.05	Antagonism
50	1	0.20	1.56	Antagonism
100	1	0.95	0.19	Synergism
1	50	0.20	4.73	Antagonism
50	50	0.96	0.74	Synergism
100	50	0.97	0.68	Synergism
1	100	0.61	4.19	Antagonism
50	100	0.96	1.38	Antagonism
100	100	0.98	1.13	Antagonism

Table. 4

Abstract: Over the past decade the science has studied synthetic photosensitizers used in photodynamic therapy (PDT) or photochemotherapy as anticancer candidates. In this context, compounds extracted from vegetable species present interesting potential in the cancer field. In our laboratory, we studied Heterophyllaea pustulata a phototoxic shrub that habit the northwest of Argentina. From this vegetal, by in vitro germination, we obtained Rubiadin and Soranjidiol, two anthraquinones that exhibited significant photocytotoxicity on human cancer cells. In addition, the fraction obtained from callus cultures allowed us to get a satisfactory content of these compounds compared to those found from the original plant. Under PDT regimen, we found that cell destruction resulted in a dose-dependent manner and occasioned apoptosis on photosensitized cells. Biochemical analysis revealed the involvement of caspase-3, PARP cleavage and DNA fragmentation in Rubiadin induced apoptosis. Moreover, Soranjidiol-PDT led to μ-calpain-induced apoptosis involving caspases-3-independent DNA fragmentation. We also showed that both anthraquinones are cytoplasmatically distributed and out of nucleus. In addition, we demonstrated a synergic cytotoxic effect when we combined them.

Our data demonstrated that Rubiadin and Soranjidiol could be further considered as natural photocytotoxic compounds against cancer cells and callus cultures are a plausible source of these anthraquinonic compounds.a

Figure

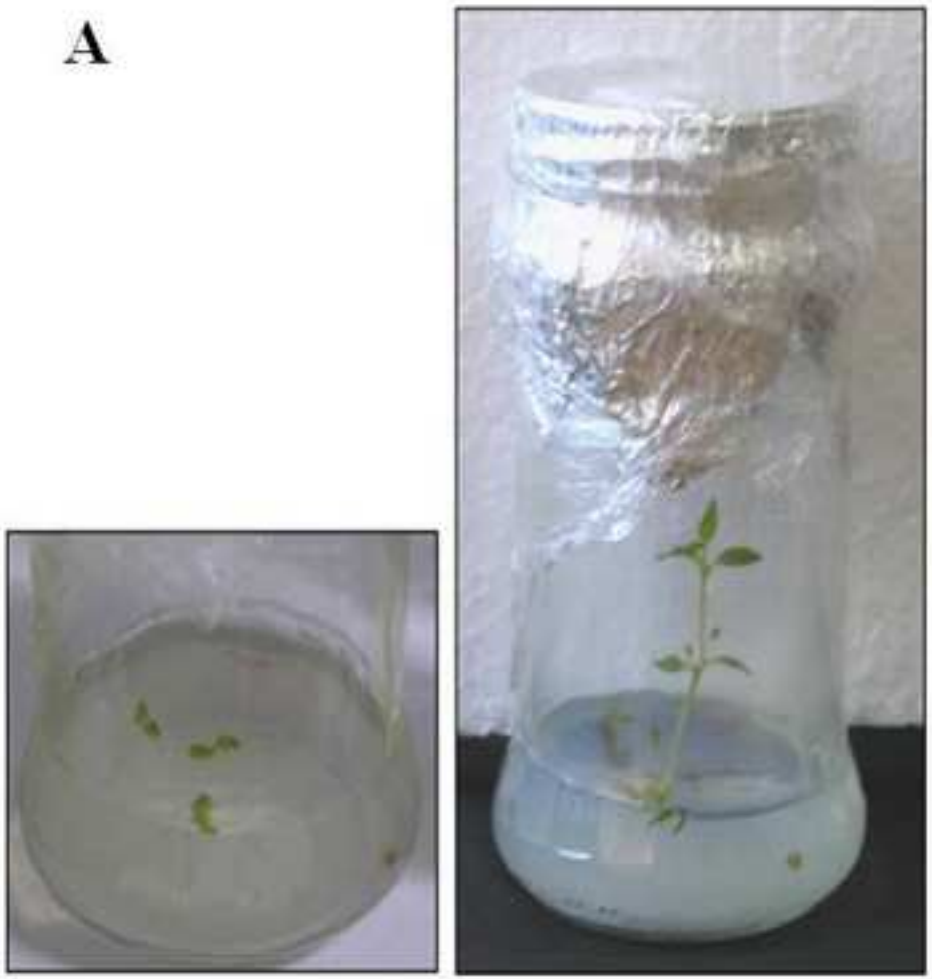

B

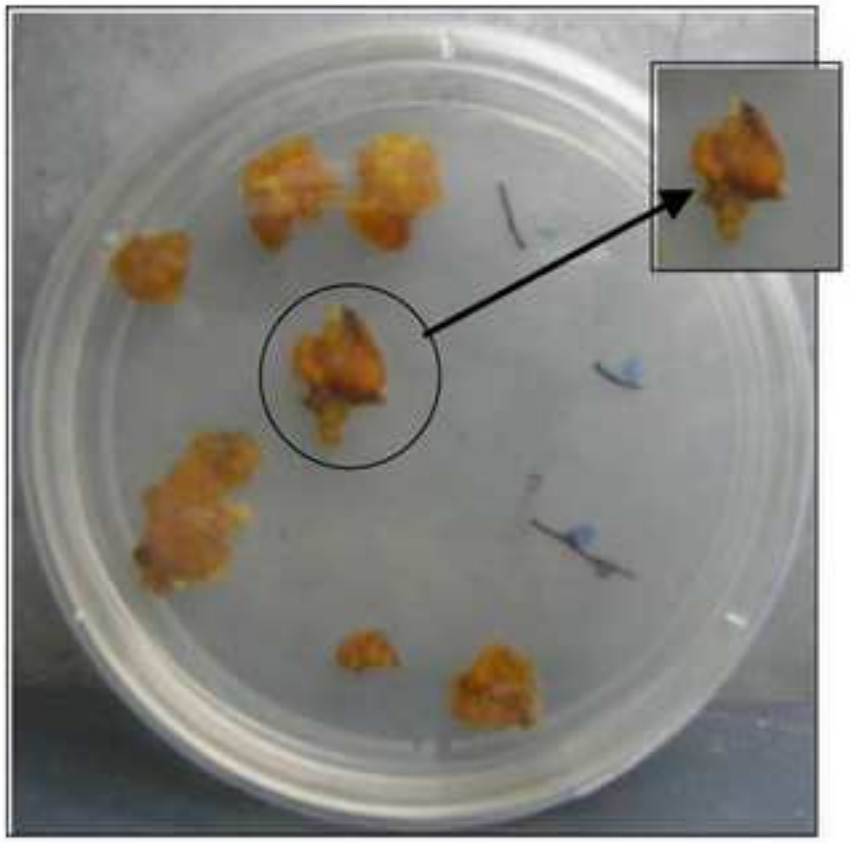

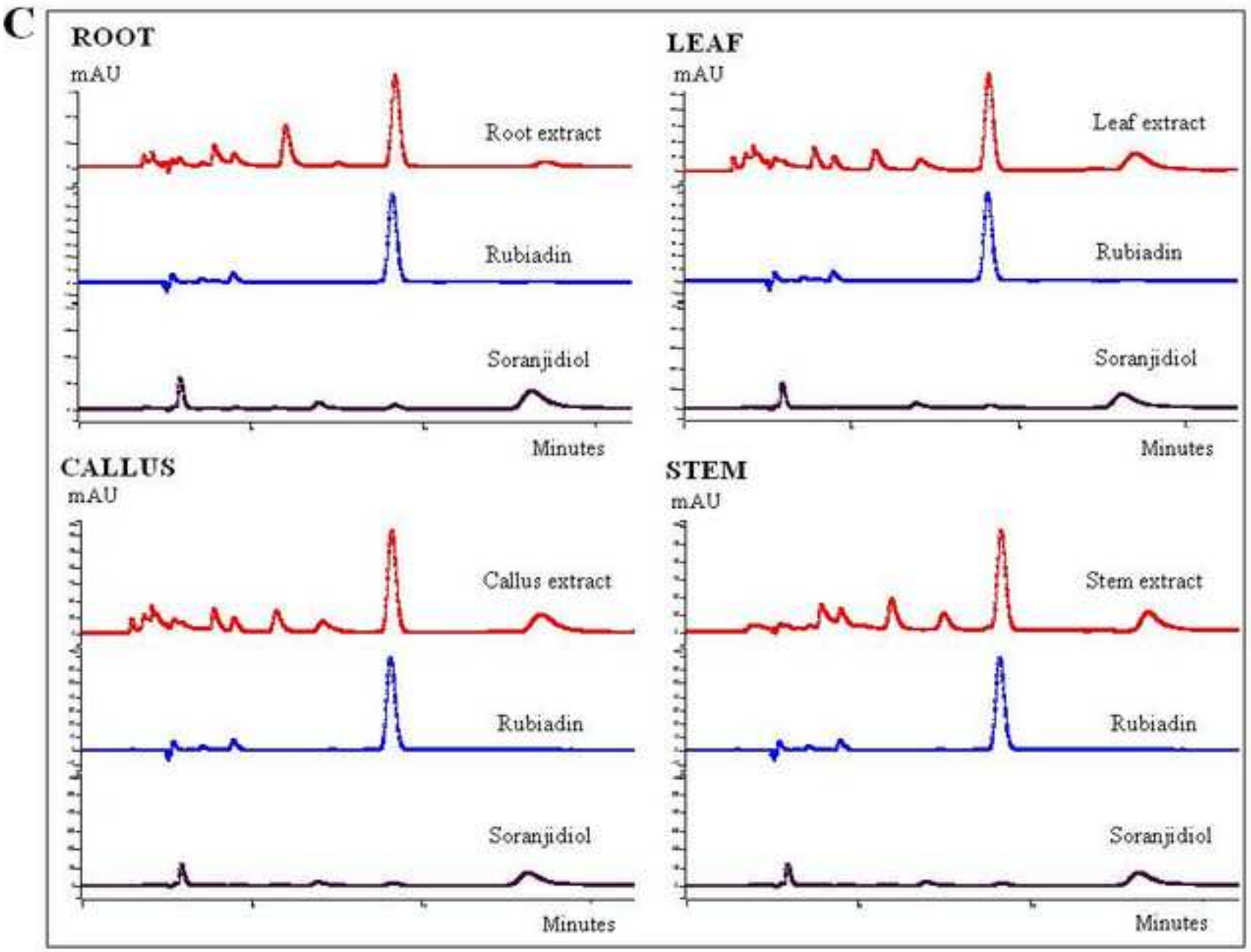
C
ROOT
mAU
Root extract
Rubiadin
Soranjidiol
Minutes
LEAF
mAU
Leaf extract
Rubiadin
Soranjidiol
Minutes
CALLUS
mAU
Callus extract
Rubiadin
Soranjidiol
Minutes
STEM
mAU
Stem extract
Rubiadin
Soranjidiol
Minutes

Figure

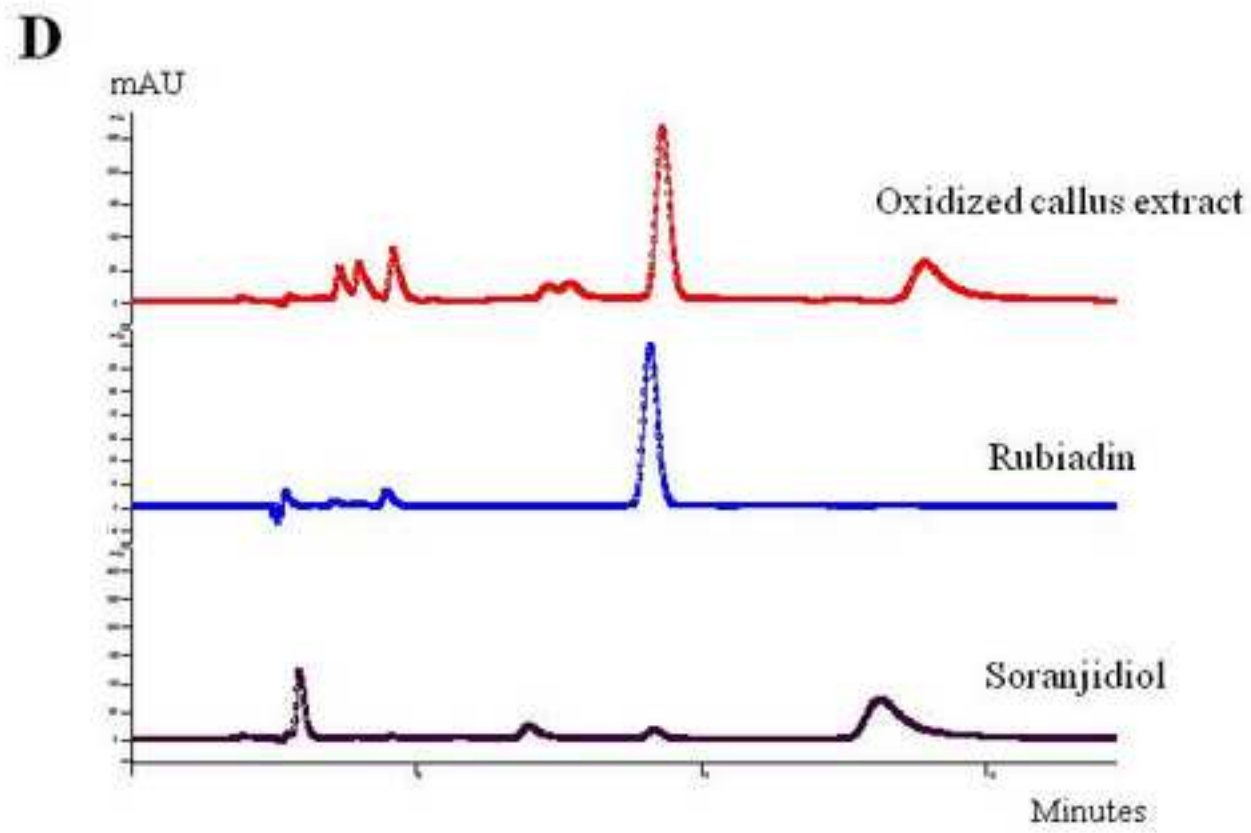
D
mAU
Oxidized callus extract
Rubiadin
Soranjidiol
Minutes

Figure

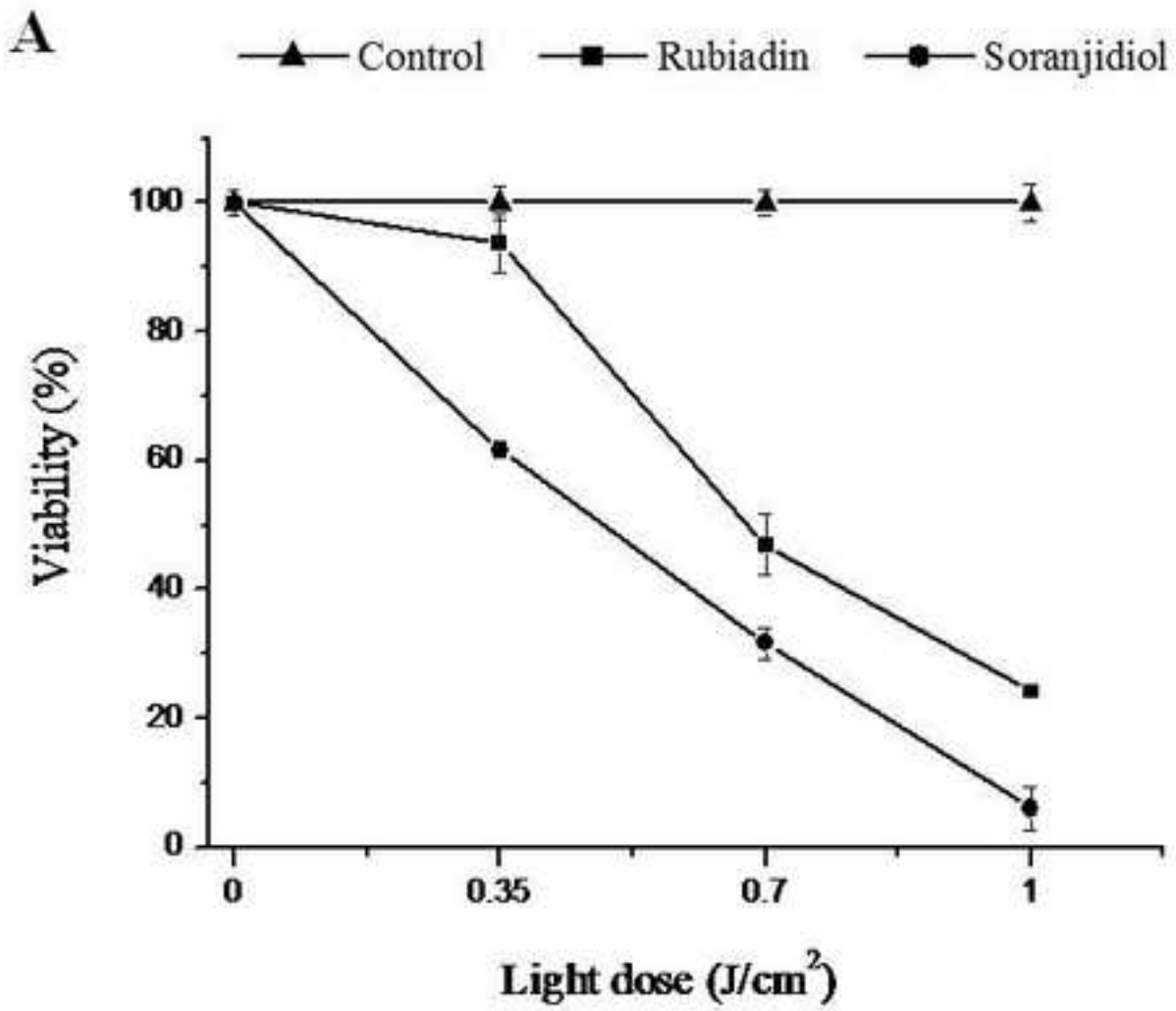
A
Control
Rubiadin
Soranjidiol
Viability (%)
100
80
60
40
20
0
0
0.35
0.7
1
Light dose (J/cm2)

Figure

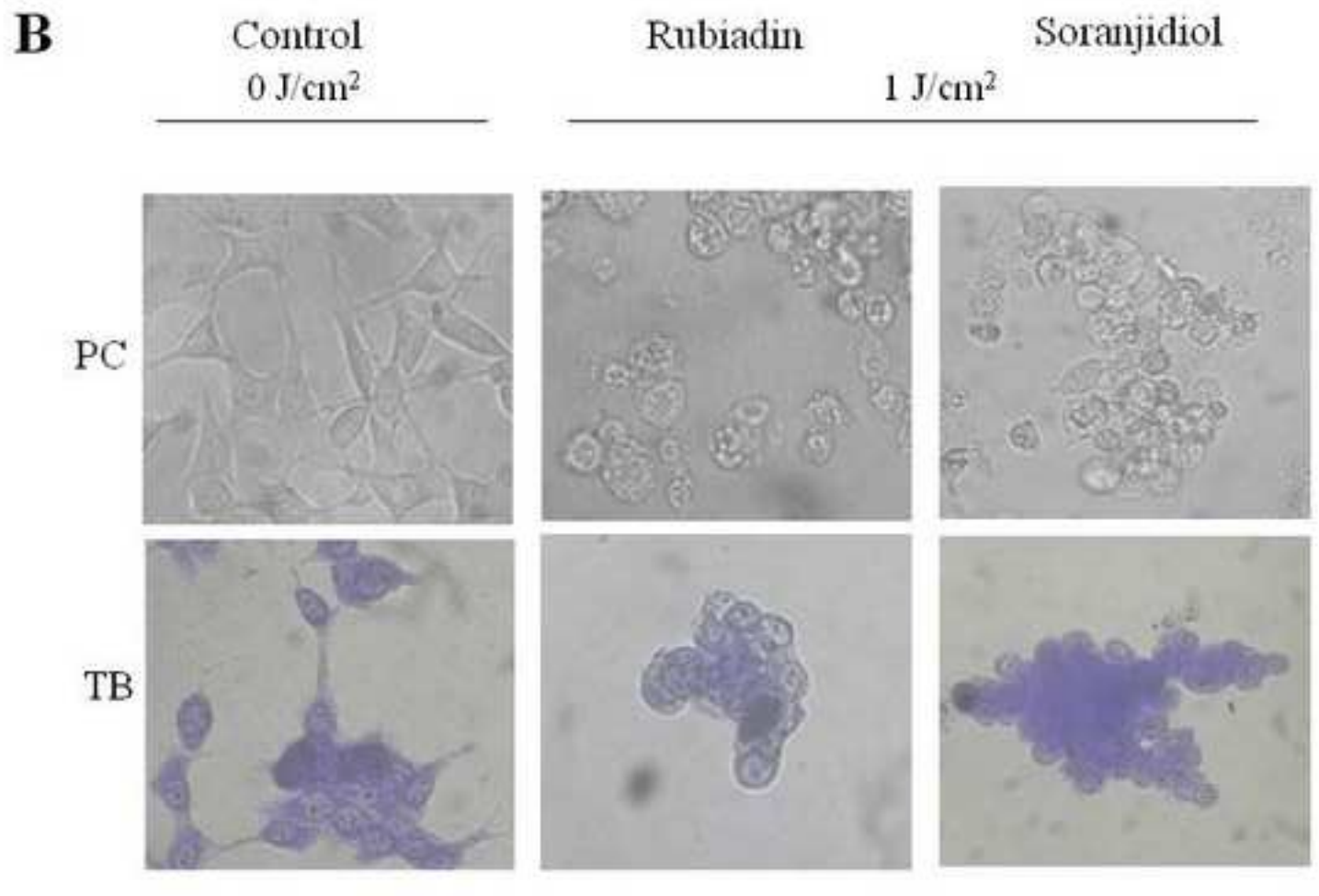

Figure

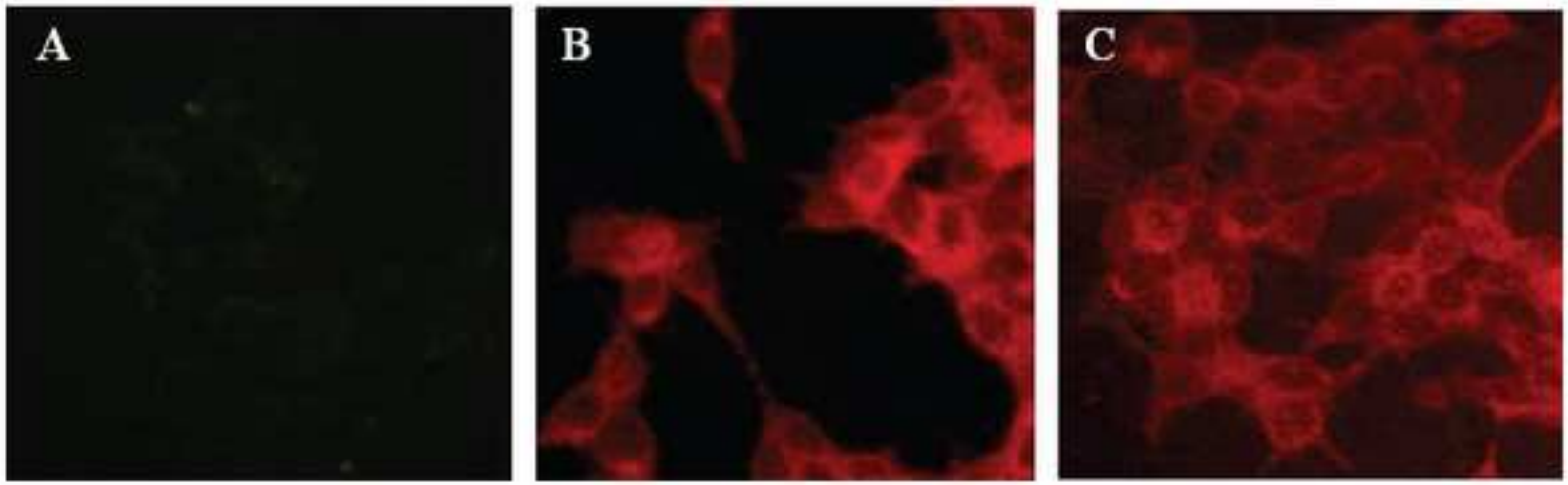

Figure

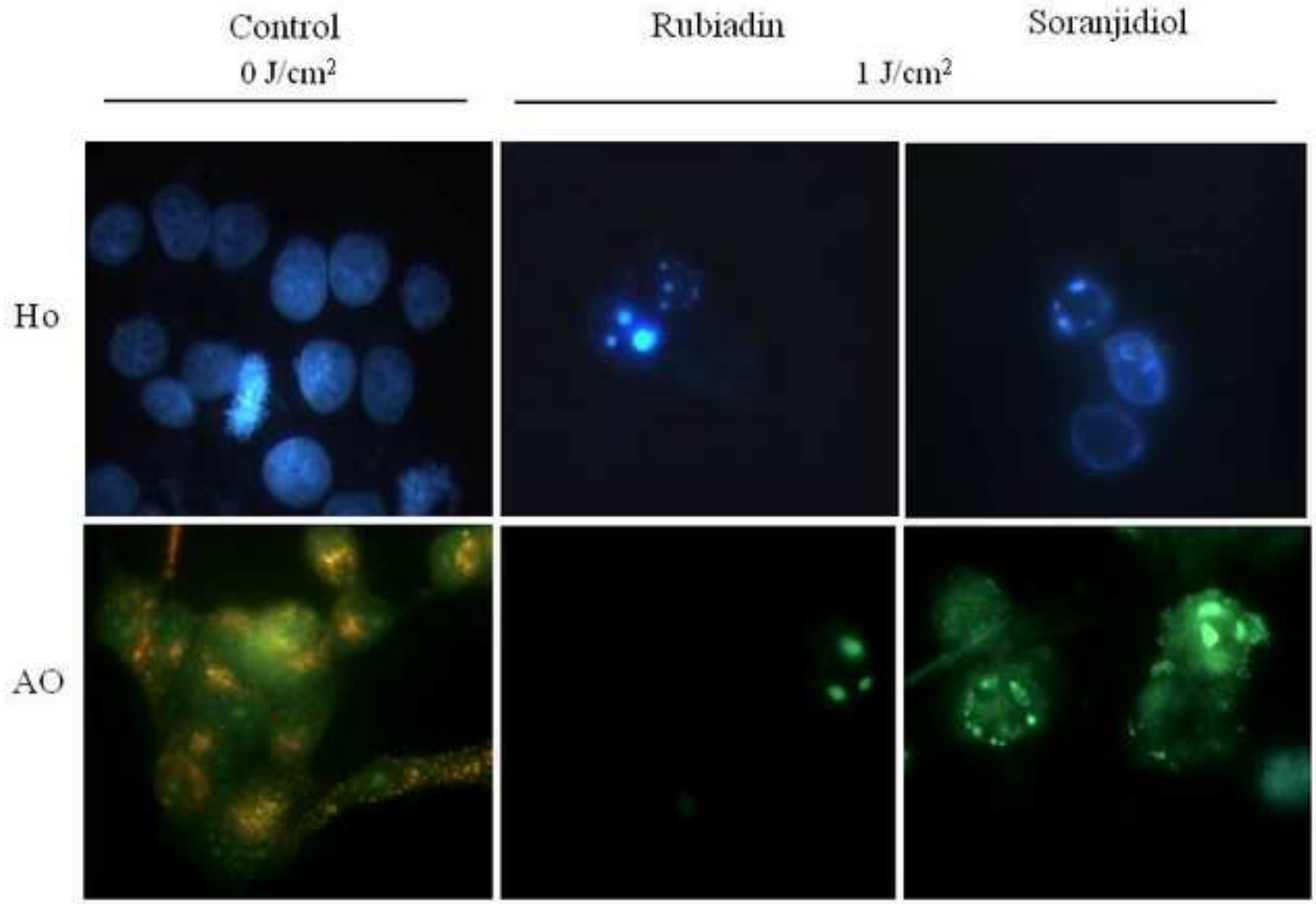

Figure

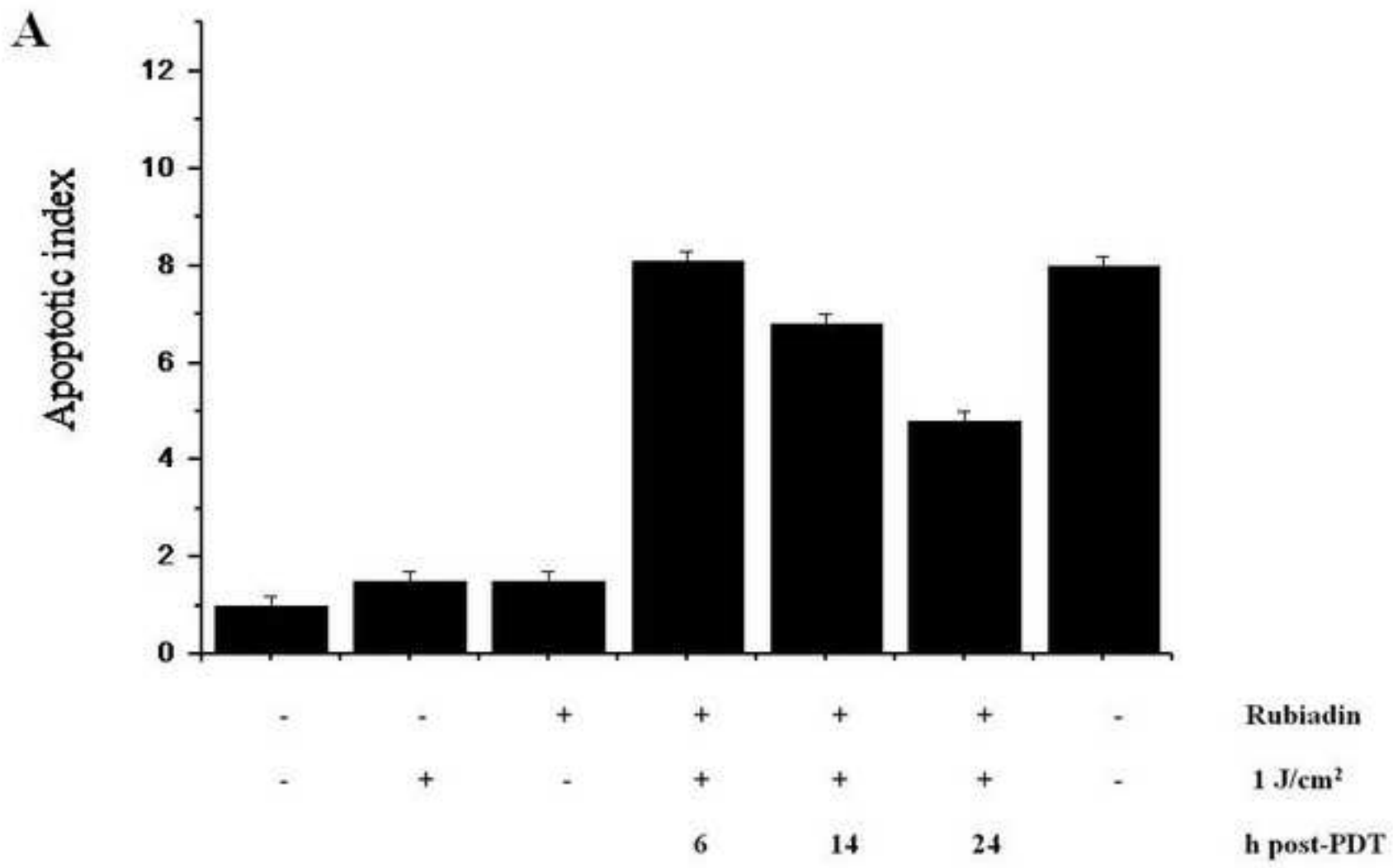
A
Apoptotic index
12
10
8
6
4
2
0
- - + + + + -
Rubiadin
- + - + + + -
1 J/cm²
6 14 24
h post-PDT

Figure

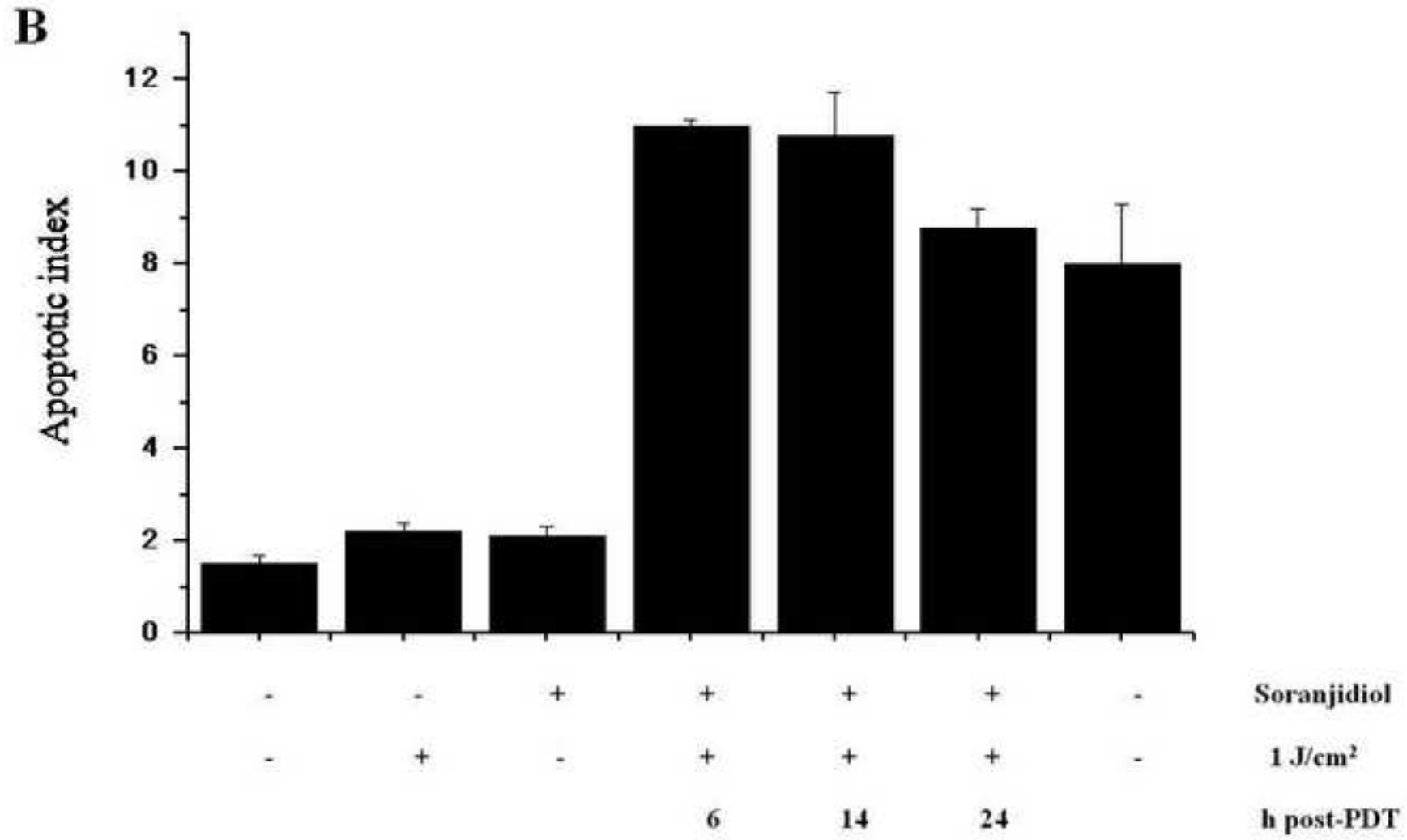
B
Apoptotic index
12
10
8
6
4
2
0
- - + + + + -
Soranjidiol
- + - + + + -
1 J/cm²
6 14 24
h post-PDT

Figure

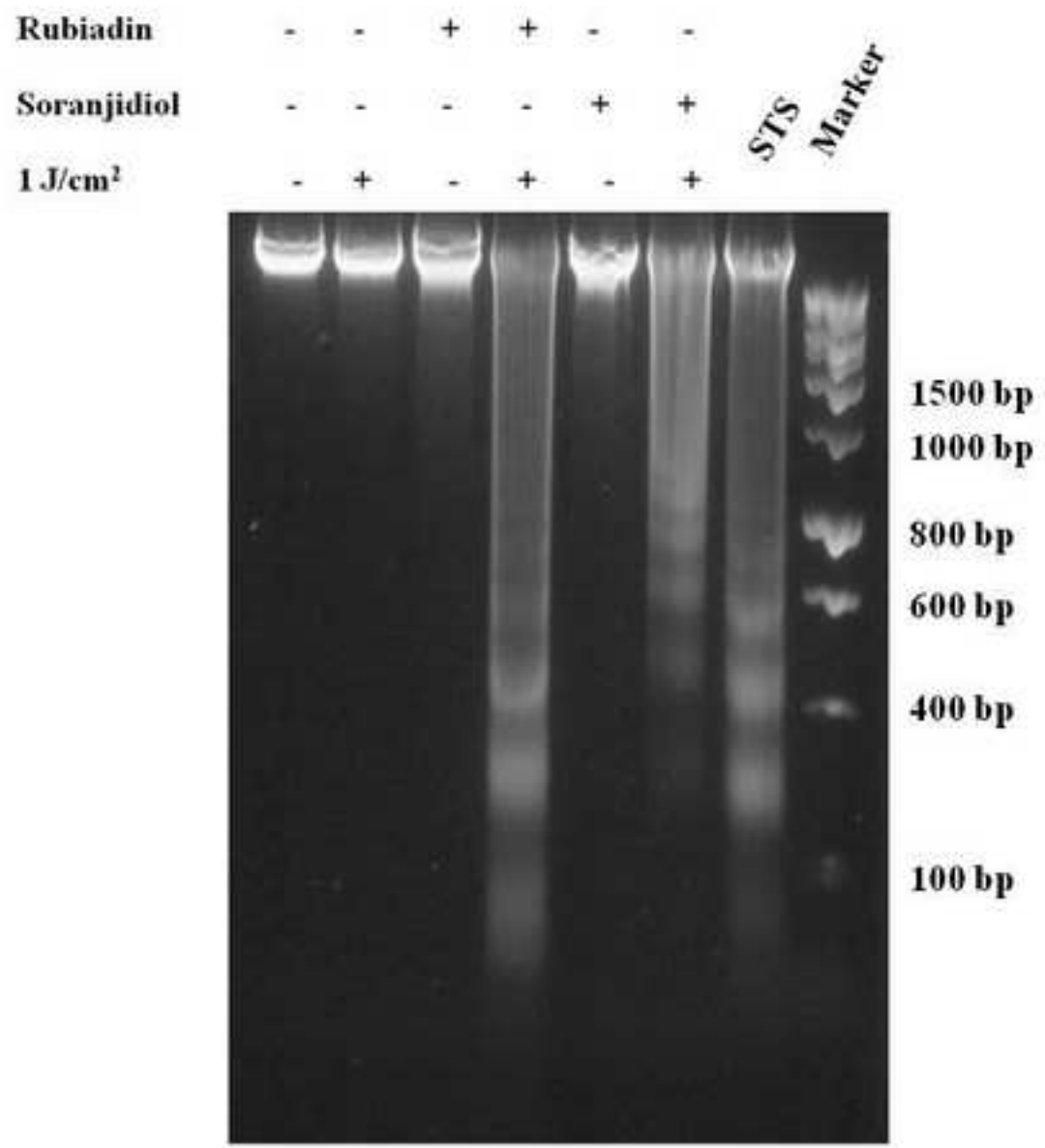
Rubiadin - - + + - -
Soranjidiol - - - - + +
1 J/cm² - + - + - +
STS
Marker
1500 bp
1000 bp
800 bp
600 bp
400 bp
100 bp

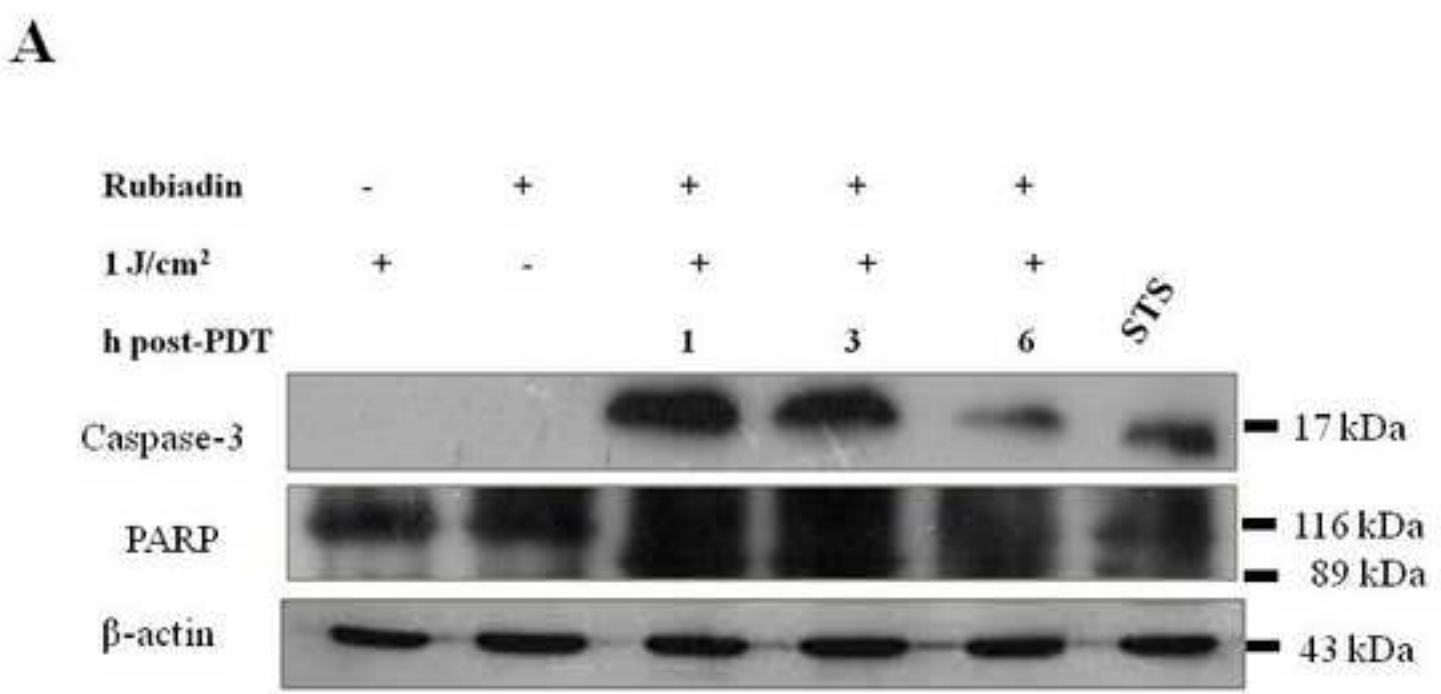
A
Rubiadin - + + + +
1 J/cm² + - + + +
h post-PDT 1 3 6 STS
Caspase-3
PARP
β-actin
17 kDa
116 kDa
89 kDa
43 kDa

Figure

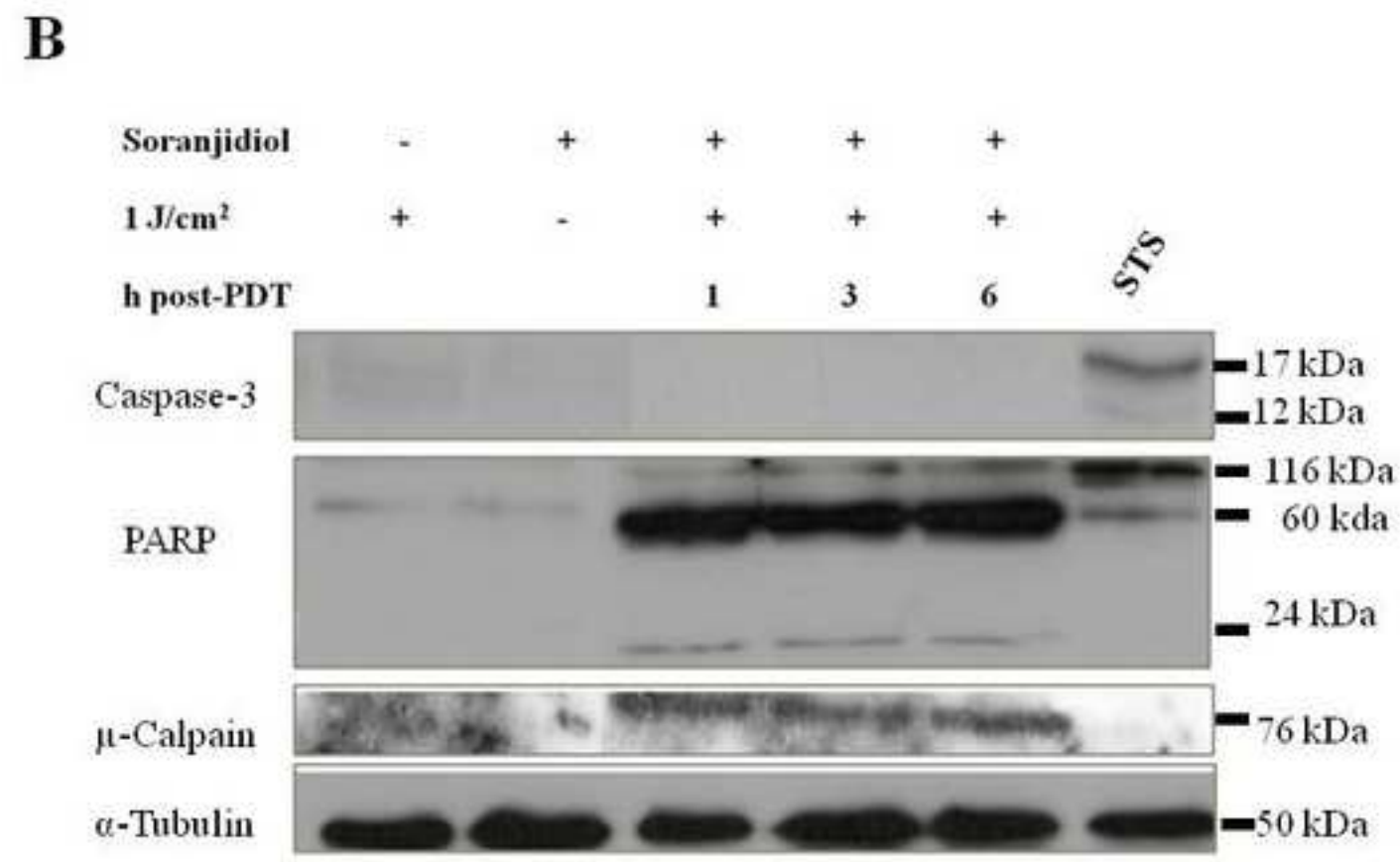
B
Soranjidiol - + + + +
1 J/cm² + - + + +
h post-PDT 1 3 6 STS
Caspase-3
17 kDa
12 kDa
PARP
116 kDa
60 kda
24 kDa
μ-Calpain
76 kDa
α-Tubulin
50 kDa

Figure

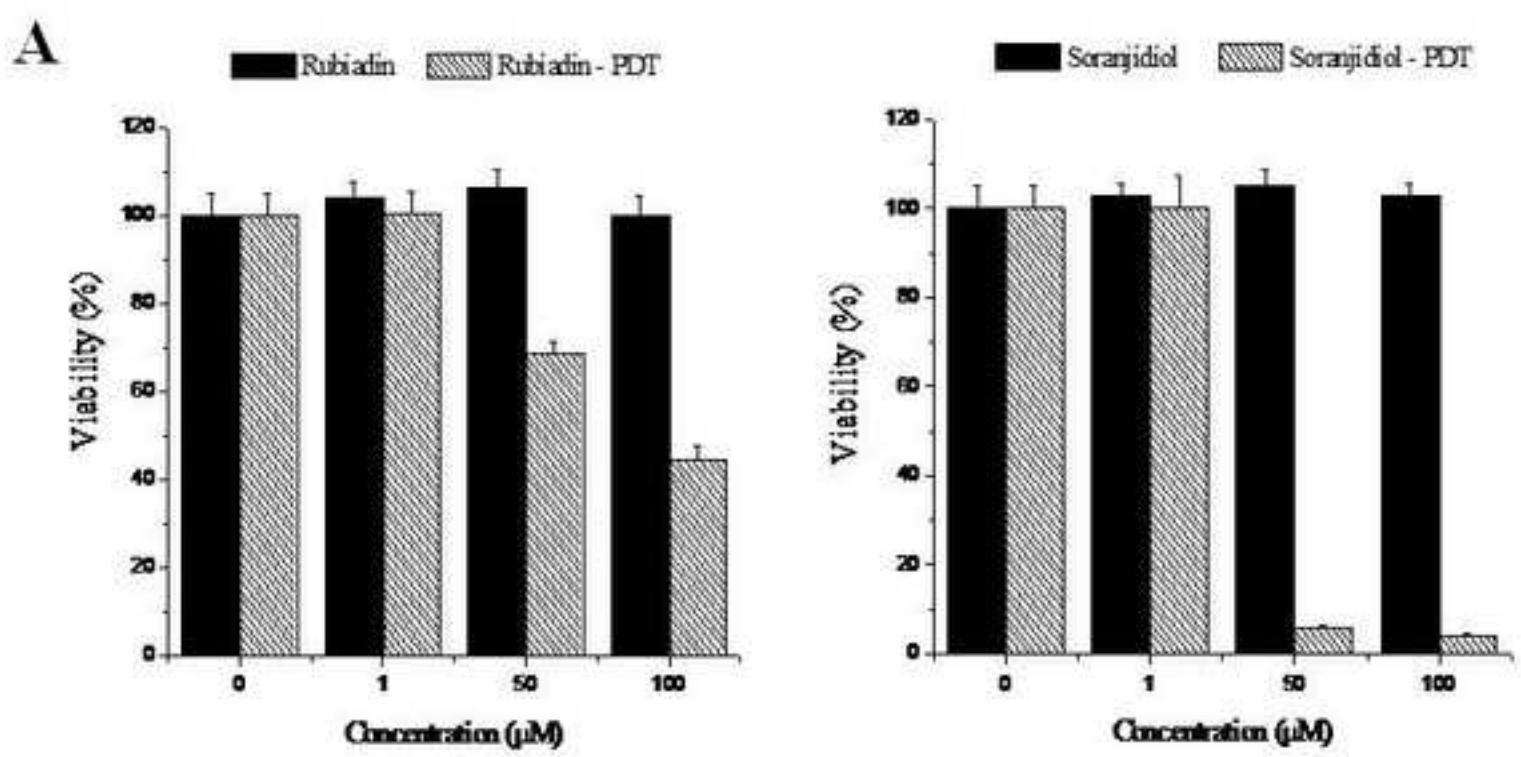
A
Rubiadin
Rubiadin - PDT
Viability (%)
120
100
80
60
40
20
0
0
1
50
100
Concentration (μM)
Soranjidiol
Soranjidiol - PDT
Viability (%)
120
100
80
60
40
20
0
0
1
50
100
Concentration (μM)

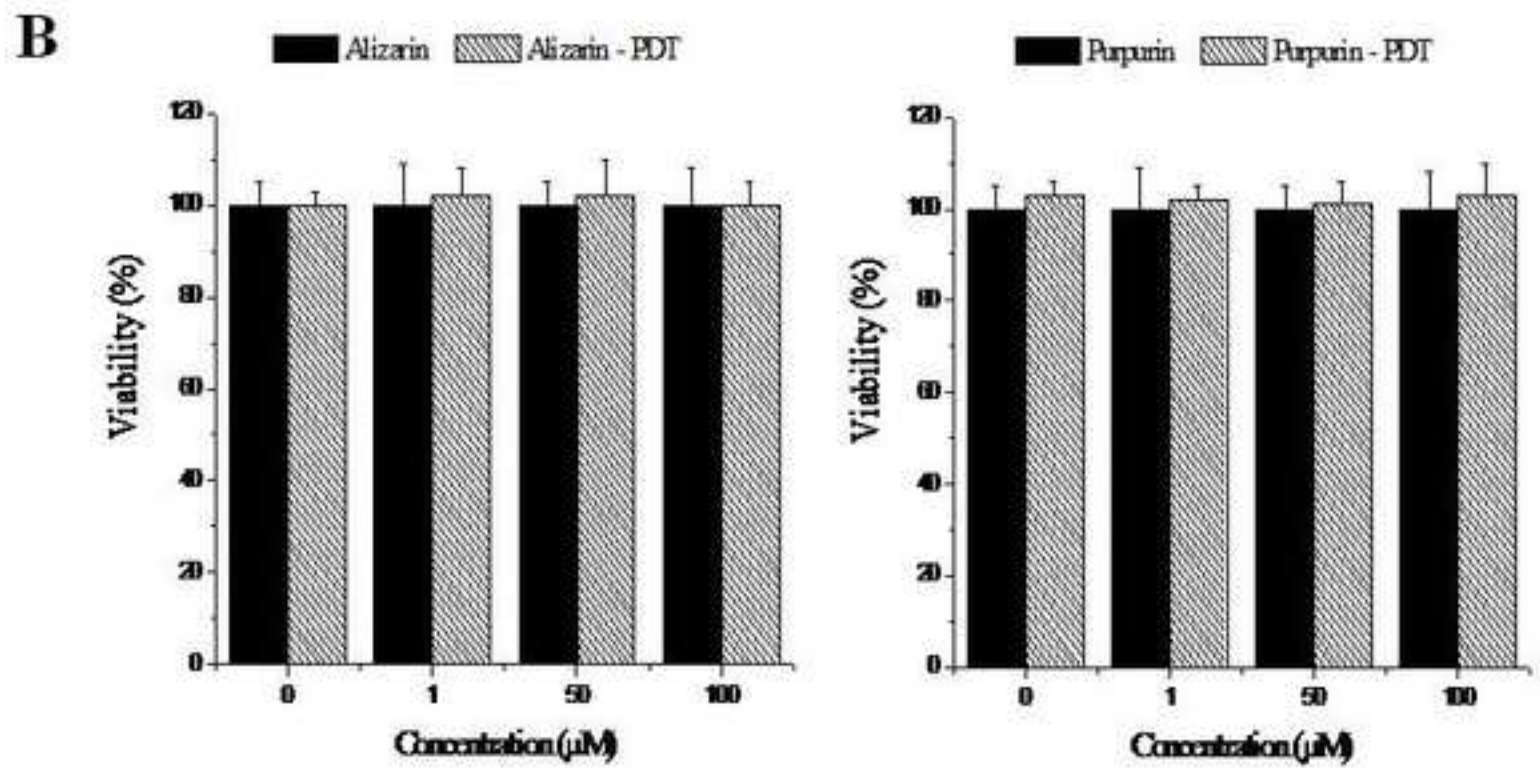
B
Alizarin
Alizarin - PDT
Viability (%)
0
20
40
60
80
100
120
0
1
50
100
Concentration (μM)
Purpurin
Purpurin - PDT
Viability (%)
0
20
40
60
80
100
120
0
1
50
100
Concentration (μM)

Figure

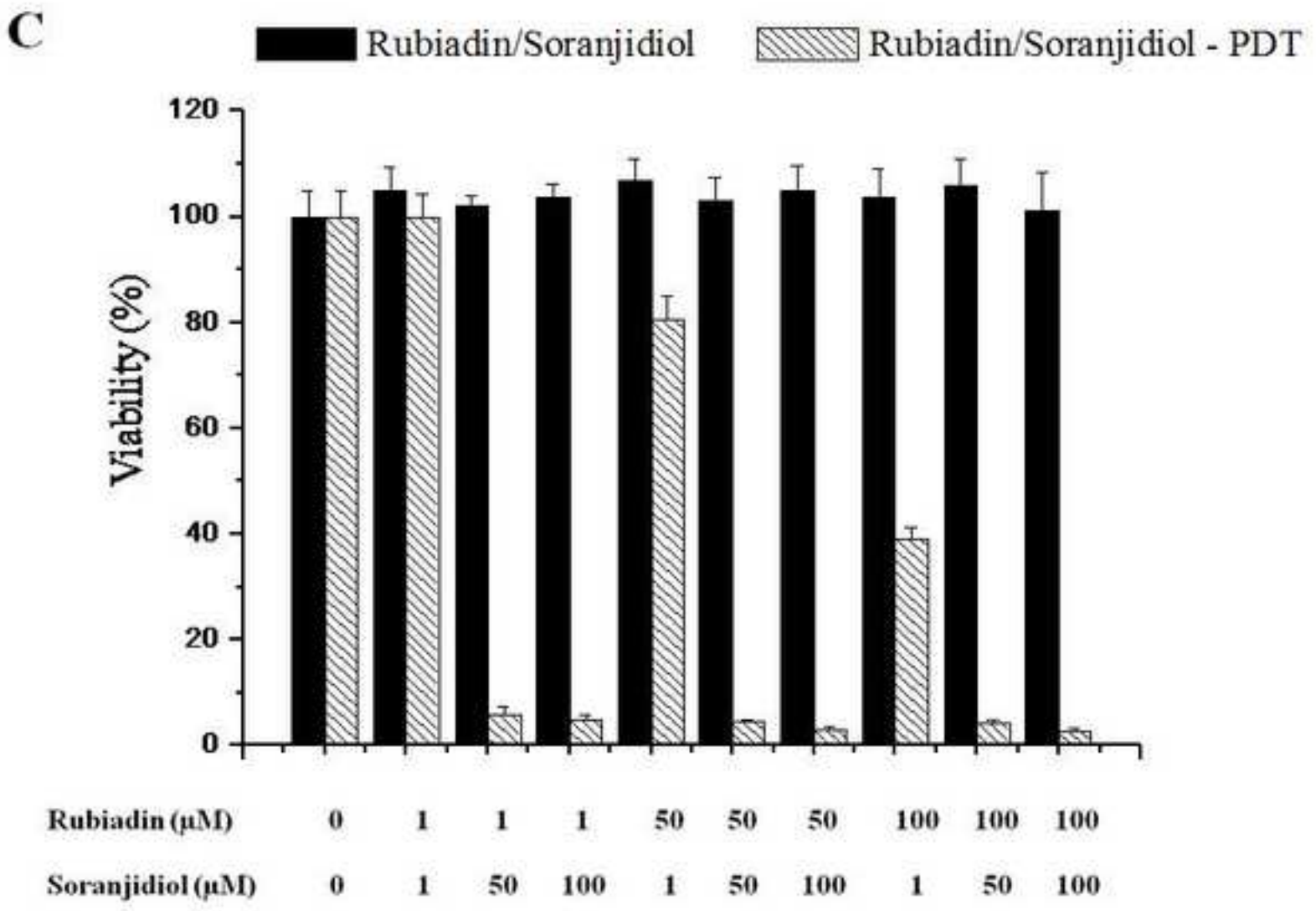
C
Rubiadin/Soranjidiol
Rubiadin/Soranjidiol - PDT
Viability (%)
120
100
80
60
40
20
0
Rubiadin (μM) 0 1 1 1 50 50 50 100 100 100
Soranjidiol (μM) 0 1 50 100 1 50 100 1 50 100